International Journal of Automotive Technology, Vol. 8, No. 3, pp. 351–359 (2007)

1229–9138/2007/034–12

HIERARCHICAL SWITCHING CONTROL OF LONGITUDINAL ACCELERATION WITH LARGE UNCERTAINTIES

F. GAO* and K.-Q. LI

State Key Laboratory of Automotive Safety and Energy, Tsinghua University, Beijing100084, China

(Received 31 August 2006; Resived 6 February 2007)

ABSTRACT–In this study, a hierarchical switching control scheme based on robust control theory is proposed for tracking control of vehicle longitudinal acceleration in the presence of large uncertainties. A model set consisting of four multiplicative-uncertainty models is set up, and its corresponding controller set is designed by the LMI approach, which can ensures the robust performance of the closed loop system under arbitray switching. Based on the model set and the controller set, a switching index function by estimating the system gain of the uncertainties between the plant and the nominal model is designed to determine when and which controller should be switched into the closed loop. After theoretical analyses, experiments have also been carried out to validate the proposed control algorithm. The results show that the control system has good performance of robust stability and tracking ability in the presence of large uncertainties. The response time is smaller than 1.5s and the max tracking error is about 0.05 m/s^2 with the step input.

KEY WORDS : Acceleration control, Multi-model, Hierarchical switching, LMI

1. INTRODUCTION

Generally, the architecture of the longitudinal control systems architecture for ASV (Advanced Safety Vehicle) has an upper level controller and a lower level one. The lower level controller, which is called an acceleration controller, determines the throttle/or brake commands required to track the desired acceleration (Rajamani and Shladover, 2001). Some achievements have been obtained with regard to designing the acceleration controller in the past years, but model errors that arise from unmodeled dynamics and parameter uncertaitines have not been considered sufficiently (Hedrick 1998; Yi and Kwon, 2001; Yi and Moon, 2004; St. Germann and Isermann, 1995; Lu and Hedrick, 2003; Lee and Kim, 2002; Hou *et al.*, 2003). Some robust or adaptive methods may work when uncertainties are sufficiently small (St. Germann and Isermann, 1995; Lu and Hedrick, 2003; Lee and Kim, 2002; Hou *et al.*, 2003), but when uncertainties are large, no single fixed-parameter controller can control satisfactorily.

The objective of this study is to make the vehicle track the desired acceleration by controlling the throttle angle in the presence of large uncertainties. Hierarchical switching control is an efficient way to deal with the control problem for a plant with large uncertainties, especially sudden changes in plant dynamics (Morse, 1996; Hespanha *et al.*, 2003; Kumpai and Jeyendran, 1997; Ippoliti and Longhi, 2004). This method uses multiple models to cover the uncertainties and the feedback controller is selected from candidate controllers according to the switching indices, but a conventional hierarchical switching control system only ensures asymptotical tracking performance and usually many more models are needed (Kumpai and Jeyendran, 1997; Ippoliti and Longhi, 2004).

In this study, a hierarchical switching control scheme based on robust control theory is proposed to control the vehicle longitudinal acceleration. To reduce the number of models by utilizing the robustness of the closed loop system, multiplicative-uncertainty models are used to cover all possible model uncertainties that arise from unmodeled dynamics and parameter uncertainties. The corresponding robust controller set is designed by the LMI approach. If the system gain of the multiplicative uncertainty between the model and the plant is the smallest, the model approximates the plant the best and the controller design based on this model can control the plant well. Thus, a switching index function (by estimating the system gain of the uncertainties) is designed to select a controller from the controller set on line. Furthermore, the robust stability and tracking ability of the proposed acceleration control system are validated by theoretical analysis and experiments.

**Corresponding author.* e-mail: gao-f01@mails.tsinghua.edu.cn

2. VEHICLE LOGNGITUDINAL DYNAMICS AND MODEL SET DESIGN

To analyze vehicle longitudinal dynamics, a full-order nonlinear vehicle longitudinal model has been built (McMahon and Hedrick, 1989). The model consists of an engine, a transmission and a drivertrain. Figure 1 shows the dynamical interactions among the above three subsystems. The output of the engine subsystem is engine torque, which is a nonlinear function of throttle angle and engine speed. A first order system is used to describe its transient processs. The transmission subsystem is responsible for transferring engine torque to the drivetrain. It is an automatic transmission with a hydraulic torque converter and a four forward transmission gearbox. The gear state is a nonlinear function of throttle angle and vehicle speed. The input of the drivetrain subsystem is the drive torque and its outputs are vehicle speed and acceleration, which are affected by road conditions and the aerodynamic drag force.

Due to the nonlinearities of engine, torque converter, etc., it is hard to use a linear model to describe the vehicle longitudinal dynamics at all conditions. To reduce the nonlinearities, an inverse model is used to calculate the throttle angle. The torque converter is assumed to be locked and for a given control acceleration u, the required engine torque can be computed as

$$T_{edes}=\frac{r}{R_d R_{g0}\eta_0}(M_0 u + C_D v^2 + M_0 g f_0) \quad (1)$$

where T_{edes} is required engine torque,
M_0 is nominal value of vehicle mass,
R_{g0} is nominal value of gearbox speed ratio,
R_d is final drive speed ratio,
η_0 is nominal value of transmission mechanical efficiency,
ω_e is engine speed,
C_D is aerodynamic drag coefficient,
g is gravity constant,
f_0 is nominal value of rolling resistance coefficient,
v is vehicle speed,
r is wheel radius.

The engine torque is a nonlinear function of ω_e and the throttle angle, θ. Typically the engine map is provided by the manufacture as a look-up table. The throttle angle for the desired engine torque at a given engine speed can be computed by the inverse engine map as follows.

$$\theta=\mathrm{MAP}^{-1}(T_{edes}, \omega_e) \quad (2)$$

where $\mathrm{MAP}^{-1}(.)$ is the inverse enginee map. Connecting the inverse model to the vehicle longitudinal model, a new plant P whose input is u and output is vehicle acceleration a is obtained as shown in Figure 2. Since the nonlinearities of the vehicle longitudinal dynamics are eliminated by the inverse model, P is considered as a linear system.

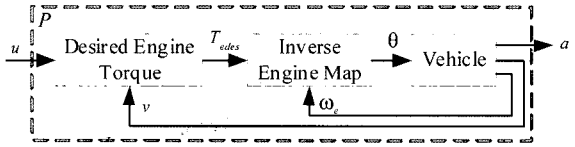

Figure 2. Linearized plant by the inverse model.

Table 1. Ranges of vehicle and environmental parameters.

Parameter	Units	Range	Nominal value
Vehicle mass	kg	1000~1500	1250
Road slope	rad	-0.1~0.1	0
Wind speed	m/s	-8~8	0
Coefficient of rolling resistance	-	0.01~0.04	0.025
Time constant of engine	s	0.2~0.5	0.35
Transmission mechanical efficiency	-	0.8~0.99	0.89
Gearbox speed ratio	-	0.74, 1, 1.44, 2.71	1.416

In practical driving conditions, the exact values of some vehicle parameters are unknown, so nominal values are used when using the inverse model to compute the throttle angle. The ranges and the nominal values of such parameters are shown in Table 1.

To obtain the dynamics of P, the parameter space in Table 1 is transformed into several discrete points. At each point, a transfer function is estimated by a process estimation method. The range of the frequency response of P is depicted in Figure 3.

For such a plant with large uncertainties, a single fixed-parameter controller can hardly ensure both robust stability and tracking performance. Thus, in this paper,

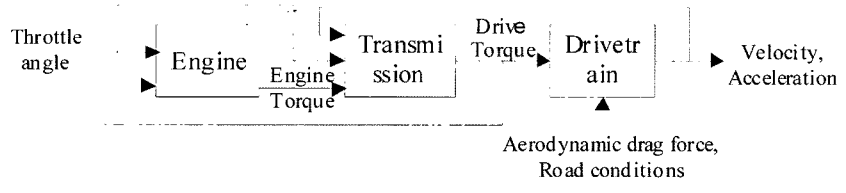

Figure 1. Structure of the vehicle longitudinal model.

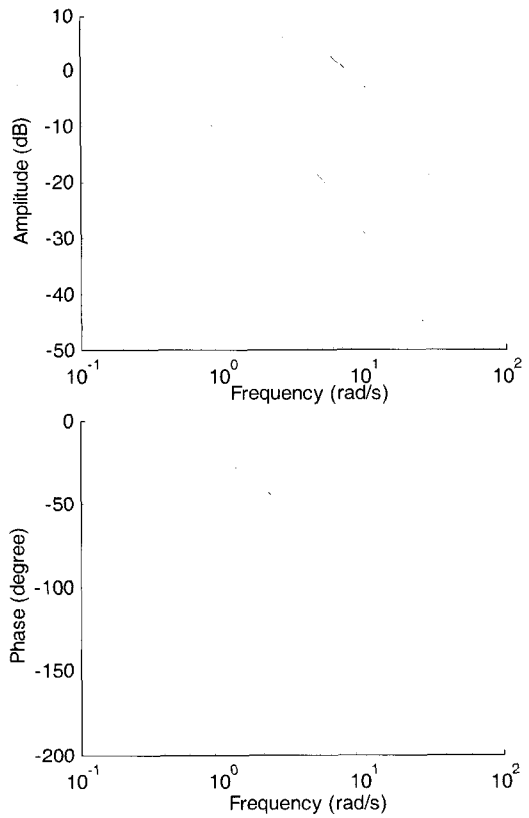

Figure 3. Ranges of the frequency response of P.

multiple multiplicative-uncertainty models are used to cover all possible uncertainties. Since the L_2 norm of a practical signal is monotone increasing, $L_{2\delta}$ norm is used to evaluate signals, which are defined as (Datta, 1998)

$$\|u\|_2^{\delta}=\sqrt{\int_0^t e^{-\delta(t-\tau)}u^T(\tau)u(\tau)d\tau} \tag{3}$$

where $\delta>0$ is a constant. Considering both the sensitivity to the noise and the adaptive speed, in this paper δ=0.4. In practice, the $L_{2\delta}$ norm can be calculated by (Morse, 1996)

$$\|u\|_2^{\delta}=\sqrt{\frac{1}{s+\delta}|u|^2} \tag{4}$$

Finally, a model set **P** consisting of four multiplicative-uncertainty models is set up by the method proposed in Rong *et al.* (2005).

$$\mathbf{P}=\{P_i=[1+\Delta_i W(s)]G_i(s),\ \|\Delta_i\|_{\infty}^{\delta}<1,\ i=1,\ \ldots,\ 4\} \tag{5}$$

where $W(s)=\dfrac{2.1s+2.478}{s+5.1}$ is the weighting function,

Δ_i is the multiplicative uncertainty,
$\|\Delta_i\|_{\infty}^{\delta}$ is induced $L_{2\delta}$ norm,
$G_i(s)$, i=1...4 is the nominal model and

$$G_1(s)=\frac{6.23}{s+3.33},\ G_2(s)=\frac{3.31}{s+3.33},$$

$$G_3(s)=\frac{2.30}{s+3.33},\ G_4(s)=\frac{1.70}{s+3.33}.$$

Based on the model set **P**, a corresponding controller set **C** and a switching algorithm will be designed in the next section.

3. HIERARCHICAL SWITCHING CONTROL SYSTEM DESIGN

The hierarchical switching acceleration control system based on uncertainty estimation is shown in Figure 4. The upper layer consists of the uncertainty estimator **E** and the switching logic **S**. The uncertainty estimator outputs the switching indices $\pi_i(t)$ by the input and output of P. The switching indices can evaluate the multiplicative uncertainty between the plant and the nominal models. The switching logic outputs the switching signal $\sigma(t)$ based on the the switching indices. $\sigma(t)$ is a piecewise-constant signal taking values in {1, 2, 3, 4}. The controller whose index equals the switching signal will be selected to control the plant. The lower layer system is made up of P and the controller set **C**. It is a linear time invariant feedback control system when $\sigma(t)$ is fixed, and switching occurs when $\sigma(t)$ changes.

3.1. Uncertainty Estimator E Design

Before designing the estimator, a simple example is given to illustrate the motivation of the proposed method. The plant is assumed to be described by a multiplicative uncertainty model as

$$y=[1+\Delta W(s)]\ G(s)u \tag{6}$$

where u and y are input and output signal, respectively. Then y can be estimated by

$$\hat{y}=\frac{D(s)}{\Lambda(s)}u+\frac{\Lambda(s)+N(s)}{\Lambda(s)}a \tag{7}$$

where $D(s)$ and $N(s)$ are polynomials and satisfy

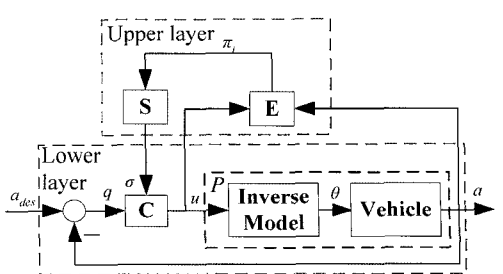

Figure 4. Hierarchical switching control system for vehicle longitudinal acceleration.

$\frac{D(s)}{N(s)}=G(s)$

$\Lambda(s)$ is a stable polynomial.

Of course, if there is no model uncertainty, $\hat{y}$ converges to y exponentially and the convergence speed is determined by the roots of $\Lambda(s)$. The estimation error, $e=\hat{y}-y$, arises from the model uncertainties and can be computed by

$$e=-\Delta\frac{D(s)}{\Lambda(s)}W(s)u \tag{8}$$

From (8), the $\boldsymbol{L}_{2\delta}$ gain of the uncertainty part can be computed by u and the output estimation error e.

Considering the above analysis, the $\boldsymbol{L}_{2\delta}$ gain of the uncertainty part between the nominal model $G_i(s)$ and the plant P can be computed by

$$a_i=\frac{k_i}{\Lambda(s)}u+\frac{\Lambda(s)-N(s)}{\Lambda(s)}a \tag{9}$$

$$z_i=\frac{k_i(s)}{\Lambda(s)}W(s)u \tag{10}$$

$$e_i=a_i-a$$

$$\pi_i(t)=(\|e_i\|_2^{\delta})^2-(\|z_i\|_2^{\delta})^2 \tag{11}$$

where a_i is the estimated acceleration based on $G_i(s)$,

e_i is the estimation error,

z_i is the estimated input of the multiplicative uncertainty,

$D_i(s)$ and $N_i(s)$ satisfy $\frac{k_i}{N(s)}=G_i(s)$,

$\Lambda(s)=s+30$ in this paper.

$\pi_i(t)$ is the swiching index, which can evaluate the $\boldsymbol{L}_{2\delta}$ gain of the model uncertainty.

(9) is the output estimator which was designed based on $G_i(s)$ and (10) estimates the input signal of the uncertainty part.(11) computes the switching index. The definition of the system $\boldsymbol{L}_{2\delta}$gain is not used to compute the switching index, since the switching index function (11) can simplify the theoretical analysis. The state-shared dynamic system of the estimator (9) and (10) is

$$\begin{bmatrix}\dot{\boldsymbol{x}}_{E1}\\ \dot{\boldsymbol{x}}_{E2}\end{bmatrix}=\begin{bmatrix}\begin{bmatrix}-30 & 0\\ 0 & -30\end{bmatrix} & 0\\ 0 & \boldsymbol{A}_{E2}\end{bmatrix}\begin{bmatrix}\boldsymbol{x}_{E1}\\ \boldsymbol{x}_{E2}\end{bmatrix}+\begin{bmatrix}\begin{bmatrix}1\\0\end{bmatrix}\\ \boldsymbol{B}_{E1}\end{bmatrix}u+\begin{bmatrix}\begin{bmatrix}0\\1\end{bmatrix}\\ 0\end{bmatrix}a$$

$$a_i=[k_i\ 26.67]\boldsymbol{x}_{E1},\ z_i=\boldsymbol{C}_{E3i}\boldsymbol{x}_{E2},\ i=1\ldots4 \tag{12}$$

where $\boldsymbol{x}_{E1}$ and $\boldsymbol{x}_{E2}$ are states of the estimator,

$$\boldsymbol{A}_{E2}=\begin{bmatrix}0 & -153\\ 1 & -35.1\end{bmatrix},\ \boldsymbol{B}_{E1}=\begin{bmatrix}1\\0\end{bmatrix}$$

$\boldsymbol{C}_{E3i}$ satisfy $\boldsymbol{C}_{E3i}(sI-\boldsymbol{A}_{E2})^{-1}\boldsymbol{B}_{E1}=\frac{k_i}{\Lambda(s)}W(s)$.

3.2. Switching Logic S Design

The motivation for this switching logic is: if the $\boldsymbol{L}_{2\delta}$ gain of the multiplicative uncertainty between one nominal model and the plant is the smallest, this nominal model approximates the plant best and the controller designed on the basis of this model should achieve the best performance. Thus, the following switching logic is used.

$$\sigma(t)=\underset{i\in\{1,2,3,4\}}{\arg\min}\{\pi_i(t)\} \tag{13}$$

For example, if $\pi_k(t)$ is smallest at time t, then $\sigma(t)$ is set to k, and the controller whose index equals k is selected to control the plant at the same time.

Before designing the controller set, the hierarchical switching control system is first transformed to a more common structure. Without loss of generality, the plant P is assumed to be described by $P_j(s)$. The initial states are assumed to be zero and the output estimation error e_j is derived from the estimator (9), (10) and the plant model.

$$\begin{aligned}e_j&=-\Delta_j\frac{D_j(s)}{\Lambda(s)}W(s)u\\ z_j&=\frac{D_j(s)}{\Lambda(s)}W(s)u\end{aligned} \tag{14}$$

Since $\|\Delta_j\|_{\infty}^{\delta}<1$, the following inequality is obtained.

$$\pi_j(t)=\left(\|e_j\|_2^{\delta}\right)^2-\left(\|z_j\|_2^{\delta}\right)^2<0 \tag{15}$$

Without loss of generality, the switching sequence is assumed to be

$$\sigma(t)=\begin{cases}\sigma_0, 0=t_0\le t\le t_1\\ \sigma_1, t_1<t\le t_2\\ \vdots\end{cases} \tag{16}$$

Since the switching indices are continuous, at the switching times we have the following equation.

$$\pi_{\sigma_i}(t_{i+1})=\pi_{\sigma_{i+1}}(t_{i+1}) \tag{17}$$

At any time $t>0$, $t\in(t_n,t_{n+1})$, the following equation is obtained.

$$\begin{aligned}&\left(\|e_\sigma\|_2^{\delta}\right)^2-\left(\|z_\sigma\|_2^{\delta}\right)^2\\ &=\int_0^t e^{-\delta(t-\tau)}e_\sigma^2(\tau)\mathrm{d}\tau-\int_0^t e^{-\delta(t-\tau)}z_\sigma^2(\tau)\mathrm{d}\tau\\ &=\int_0^{t_1}e^{-\delta(t-\tau)}e_{\sigma_0}^2(\tau)\mathrm{d}\tau+\cdots+\int_{t_n}^{t}e^{-\delta(t-\tau)}e_{\sigma_n}^2(\tau)\mathrm{d}\tau\\ &-\left(\int_0^{t_1}e^{-\delta(t-\tau)}z_{\sigma_0}^2(\tau)\mathrm{d}\tau+\cdots+\int_{t_n}^{t}e^{-\delta(t-\tau)}z_{\sigma_n}^2(\tau)\mathrm{d}\tau\right)\end{aligned} \tag{18}$$

Between two switchings, we have the following equation.

$$\begin{aligned}&\int_{t_i}^{t_{i+1}} e^{-\delta(t-\tau)}\left[e_{\sigma_i}^2(\tau)-z_{\sigma_i}^2(\tau)\right]d\tau\\&=\int_0^{t_{i+1}} e^{-\delta(t-\tau)}\left[e_{\sigma_i}^2(\tau)-z_{\sigma_i}^2(\tau)\right]d\tau\\&-\int_0^{t_i} e^{-\delta(t-\tau)}\left[e_{\sigma_i}^2(\tau)-z_{\sigma_i}^2(\tau)\right]d\tau\\&=e^{-\delta(t-t_{i+1})}\pi_{\sigma_i}(t_{i+1})-e^{-\delta(t-t_i)}\pi_{\sigma_i}(t_i)\end{aligned} \tag{19}$$

Substituting (19) to (18) yields

$$\begin{aligned}&\left(\|e_\sigma\|_2^\delta\right)^2-\left(\|z_\sigma\|_2^\delta\right)^2\\&=e^{-\delta(t-t_1)}\pi_{\sigma_0}(t_1)-\left[e^{-\delta(t-t_1)}\pi_{\sigma_1}(t_1)-e^{-\delta(t-t_2)}\pi_{\sigma_1}(t_2)\right]\\&-\cdots-\left[e^{-\delta(t-t_n)}\pi_{\sigma_n}(t_n)-\pi_{\sigma_n}(t)\right]\end{aligned} \tag{20}$$

Substituting (17) to (20) yields

$$\left(\|e_\sigma\|_2^\delta\right)^2-\left(\|z_\sigma\|_2^\delta\right)^2=\pi_{\sigma_n}(t) \tag{21}$$

According to the switching logic described in Section B, we have the following inequality.

$$\pi_{\sigma_n}(t)<\pi_j(t)<0 \tag{22}$$

From (22), the upper system shown in Fig. 4 confirms that the $L_{2\delta}$ gain from signal z_σ to e_σ is smaller than 1.

Substituting $a=a_\sigma-e_\sigma$ into the estimator (12), the plant P can be replaced by the following uncertain switching system.

$$\begin{bmatrix}\dot{x}_{E1}\\ \dot{x}_{E2}\end{bmatrix}=\begin{bmatrix}\begin{bmatrix}-30 & 0\\ k_\sigma & -3.33\end{bmatrix} & 0\\ 0 & A_{E2}\end{bmatrix}\begin{bmatrix}x_{E1}\\ x_{E2}\end{bmatrix}+\begin{bmatrix}\begin{bmatrix}1\\0\end{bmatrix}\\ B_{E1}\end{bmatrix}u-\begin{bmatrix}\begin{bmatrix}0\\1\end{bmatrix}\\ 0\end{bmatrix}e_\sigma \tag{23}$$
$$a=\begin{bmatrix}k_\sigma & 26.67\end{bmatrix}x_{E1}-e_\sigma,\ z_\sigma=C_{E3\sigma}x_{E2}$$

In the switching system (23), e_σ is a disturbance arising from the uncertainty part and z_σ is an input of the uncertainty part. The plant is equivalent to the switching system depicted in Figure 5. Δ is considered as the uncertainty part of the switching system $\Sigma_{\sigma(t)}$, which is described by (23). From the above analysis, we know the $L_{2\delta}$ gain from z_σ to e_σ is smaller than 1. a_{des} is the desired acceleration and the signal $q=a_{des}-a$ is the tracking error. $W_p(s)$ is the performance weighting function and $W_{per}(s)=\dfrac{0.1s+1.1}{s}$ in this paper.

3.3. Controller set C Design

The objective of the controller set design is to make the $L_{2\delta}$ gain from a_{des} to q^* smaller than γ in the presence of the uncertainties Δ, which ensures the robust performance. Before proceeding, a lemma, which is very useful for the controller set design, is introduced first.

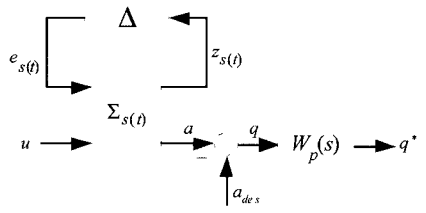

Figure 5. Equivalent switching system of the plant.

Lemma 1: For the following switching system

$$\begin{aligned}\dot{x}&=A_\sigma x+B_{1\sigma}w_1+B_{2\sigma}u+B_{3\sigma}w_2\\z_1&=C_{1\sigma}x+D_{11\sigma}w_1+D_{12\sigma}u+D_{13\sigma}w_2\\z_2&=C_{2\sigma}x+D_{21\sigma}w_1+D_{22\sigma}u+D_{23\sigma}w_2\\z_1&=\Delta w_1\end{aligned} \tag{24}$$

where σ is the switching signal and takes values in Ω, and Δ is the uncertainty part and satisfies

$$\|\Delta\|_\infty^\delta<\frac{1}{\beta} \tag{25}$$

If there exist symmetric positive definite matrix X and matrix Y_i, $i\in\Omega$, which satisfy the following linear matrix inequality (26).

$$\begin{bmatrix}\left(A_i^\delta X+B_{2i}Y_i\right)^{\mathrm{T}}+\left(A_i^\delta X+B_{2i}Y_i\right) & B_{1i} & B_{3i}\\ B_{1i}^{\mathrm{T}} & -\beta^2 I & 0\\ B_{3i}^{\mathrm{T}} & 0 & -\gamma^2 I\\ C_{1i}X+D_{12i}Y_i & D_{11i} & D_{13i}\\ C_{2i}X+D_{12i}Y_i & D_{21i} & D_{23i}\end{bmatrix}$$
$$\begin{bmatrix}\left(C_{1i}X+D_{12i}Y_i\right)^{\mathrm{T}} & \left(C_{2i}X+D_{12i}Y_i\right)^{\mathrm{T}}\\ D_{11i}^{\mathrm{T}} & D_{21i}^{\mathrm{T}}\\ D_{13i}^{\mathrm{T}} & D_{23i}^{\mathrm{T}}\\ -I & 0\\ 0 & -I\end{bmatrix}<0 \tag{26}$$

where $A_i^\delta=A_i+0.5\delta I$, then under arbitrary switching, the $L_{2\delta}$ gain from w_2 to z_2 is smaller than γ of the switching system (24) in the presence of the uncertainty part Δ with the following state feedback law

$$u=K_\sigma x \tag{27}$$

where $K_i=Y_iX^{-1}$, $i\in\Omega$.

Proof: Substituting the state feedback law (27) into the switching system (24) yields

$$\begin{aligned}\dot{x}&=\left(A_\sigma+B_{2\sigma}Y_\sigma X^{-1}\right)x+B_{1\sigma}w_1+B_{3\sigma}w_2\\z_1&=\left(C_{1\sigma}+D_{12\sigma}Y_\sigma X^{-1}\right)x+D_{11\sigma}w_1+D_{13\sigma}w_2\\z_2&=\left(C_{2\sigma}+D_{22\sigma}Y_\sigma X^{-1}\right)x+D_{21\sigma}w_1+D_{23\sigma}w_2\end{aligned} \tag{28}$$

The left side of the linear matrix inequality (26) is multiplied by **diag**(X^{-1}, I, I, I, I) on both sides and we have the inequality (29).

$$\begin{bmatrix} \left(A_i^{\delta}+B_{2i}Y_i X^{-1}\right)^{\mathrm{T}} X^{-1}+X^{-1}\left(A_i^{\delta}+B_{2i}Y_i X^{-1}\right) & X^{-1}B_{1i} \\ B_{1i}^{\mathrm{T}}X^{-1} & -\beta^2 I \\ B_{3i}^{\mathrm{T}}X^{-1} & 0 \\ C_{1i}+D_{12i}Y_i X^{-1} & D_{11i} \\ C_{2i}+D_{12i}Y_i X^{-1} & D_{21i} \end{bmatrix}$$

$\forall i \in \Omega$

$$\begin{bmatrix} X^{-1}B_{3i} & \left(C_{1i}+D_{12i}Y_i X^{-1}\right)^{\mathrm{T}} & \left(C_{2i}+D_{12i}Y_i X^{-1}\right)^{\mathrm{T}} \\ 0 & D_{11i}^{\mathrm{T}} & D_{21i}^{\mathrm{T}} \\ -\gamma^2 I & D_{13i}^{\mathrm{T}} & D_{23i}^{\mathrm{T}} \\ D_{13i} & -I & 0 \\ D_{23i} & 0 & -I \end{bmatrix} < 0 \tag{29}$$

By (29) and the Schur complement property (Li, 2002), we have

$$\begin{bmatrix} \left(A_i^{\delta}+B_{2i}Y_i X^{-1}\right)^{\mathrm{T}} X^{-1}+X^{-1}\left(A_i^{\delta}+B_{2i}Y_i X^{-1}\right) \\ B_{1i}^{\mathrm{T}}X^{-1} \\ B_{3i}^{\mathrm{T}}X^{-1} \end{bmatrix} \begin{bmatrix} X^{-1}B_{1i} & X^{-1}B_{3i} \\ -\beta^2 I & 0 \\ 0 & -\gamma^2 I \end{bmatrix} + \begin{bmatrix} \left(C_{1i}+D_{12i}Y_i X^{-1}\right)^{\mathrm{T}} & \left(C_{2i}+D_{12i}Y_i X^{-1}\right)^{\mathrm{T}} \\ D_{11i}^{\mathrm{T}} & D_{21i}^{\mathrm{T}} \\ D_{13i}^{\mathrm{T}} & D_{23i}^{\mathrm{T}} \end{bmatrix} \begin{bmatrix} C_{1i}+D_{12i}Y_i X^{-1} & D_{11i} & D_{13i} \\ C_{2i}+D_{12i}Y_i X^{-1} & D_{21i} & D_{23i} \end{bmatrix} < 0 \tag{30}$$

$, \forall i \in \Omega$

The left side of the linear matrix inequality (30) is represented by Ψ_i. The switching sequence is assumed to be described by (16). Between any two switching times and any time $t>0$, we have

$$\left(e^{-0.5\delta(t-\tau)}\begin{bmatrix} x(\tau) \\ w_1(\tau) \\ w_2(\tau) \end{bmatrix}\right)^{\mathrm{T}} \Psi_{\sigma_i} \left(e^{-0.5\delta(t-\tau)}\begin{bmatrix} x(\tau) \\ w_1(\tau) \\ w_2(\tau) \end{bmatrix}\right) < 0 \tag{31}$$

$\tau \in [t_i, t_{i+1}]$.

By (28) and (31), we have

$$\begin{aligned} &\frac{\mathrm{d}}{\mathrm{d}\tau}V(\tau)+\mathrm{e}^{-\delta(t-\tau)}\left(\left|z_2(\tau)\right|^2-\gamma^2\left|w_2(\tau)\right|^2\right) \\ &<\mathrm{e}^{-\delta(t-\tau)}\left(\beta^2\left|w_1(\tau)\right|^2-\left|z_1(\tau)\right|^2\right) \end{aligned} \tag{32}$$

where $V(\tau)=\mathrm{e}^{-\delta(t-\tau)}\left[x(\tau)\right]^{\mathrm{T}} X^{-1}\left[x(\tau)\right]$. During two switching times, we have the following inequality.

$$\begin{aligned} &\int_{t_i}^{t_{i+1}} \mathrm{e}^{-\delta(t-\tau)}\left[\left|z_2(\tau)\right|^2-\gamma^2\left|w_2(\tau)\right|^2\right]\mathrm{d}\tau \\ &=\int_{t_i}^{t_{i+1}}\left[\mathrm{e}^{-\delta(t-\tau)}\left(\left|z_2(\tau)\right|^2-\gamma^2\left|w_2(\tau)\right|^2\right)+\frac{\mathrm{d}}{\mathrm{d}\tau}V(\tau)\right]\mathrm{d}\tau \\ &-V\left(t_{i+1}\right)+V\left(t_i\right) \end{aligned} \tag{33}$$

Substituting (32) to (33) yields

$$\begin{aligned} &\int_{t_i}^{t_{i+1}} \mathrm{e}^{-\delta(t-\tau)}\left[\left|z_2(\tau)\right|^2-\gamma^2\left|w_2(\tau)\right|^2\right]\mathrm{d}\tau \\ &<\int_{t_i}^{t_{i+1}} \mathrm{e}^{-\delta(t-\tau)}\left[\beta^2\left|w_1(\tau)\right|^2-\left|z_1(\tau)\right|^2\right]\mathrm{d}\tau-V\left(t_{i+1}\right)+V\left(t_i\right) \end{aligned} \tag{34}$$

Defining $J=\int_0^t \mathrm{e}^{-\delta(t-\tau)}\left(\left|z_2(\tau)\right|^2-\left|w_2(\tau)\right|^2\right)\mathrm{d}\tau$, we have

$$\begin{aligned} J&=\int_{t_0}^{t_1} \mathrm{e}^{-\delta(t-\tau)}\left(\left|z_2(\tau)\right|^2-\left|w_2(\tau)\right|^2\right)\mathrm{d}\tau \\ &+\cdots+\int_{t_n}^{t} \mathrm{e}^{-\delta(t-\tau)}\left(\left|z_2(\tau)\right|^2-\left|w_2(\tau)\right|^2\right)\mathrm{d}\tau \end{aligned} \tag{35}$$

Substituting (34) to (35) yields

$$\begin{aligned} J&<\int_{t_0}^{t_1} \mathrm{e}^{-\delta(t-\tau)}\left[\beta^2\left|w_1(\tau)\right|^2-\left|z_1(\tau)\right|^2\right]\mathrm{d}\tau+\cdots+ \\ &\int_{t_n}^{t} \mathrm{e}^{-\delta(t-\tau)}\left[\beta^2\left|w_1(\tau)\right|^2-\left|z_1(\tau)\right|^2\right]\mathrm{d}\tau+V\left(t_0\right)-V(t) \end{aligned} \tag{36}$$

Since $\|\Delta\|_{\infty}^{\delta}<\frac{1}{\beta}$, we have the following inequality

$$\int_0^t \mathrm{e}^{-\delta(t-\tau)}\left[\beta^2\left|w_1(\tau)\right|^2-\left|z_1(\tau)\right|^2\right]\mathrm{d}\tau<0. \tag{37}$$

Substituting (37) to (36) yields

$$\begin{aligned} &J<\int_0^t \mathrm{e}^{-\delta(t-\tau)}\left[\beta^2\left|w_1(\tau)\right|^2-\left|z_1(\tau)\right|^2\right]\mathrm{d}\tau \\ &+V\left(t_0\right)-V(t)<V\left(t_0\right)-V(t) \end{aligned} \tag{38}$$

The initial states are assumed to be zero and, from (38), it is concluded that under arbitrary switching the $L_{2\delta}$ gain from w_2 to z_2 is smaller than γ in the presence of the uncertainty part.

By Lemma 1, the controller set design problem is equivalent to the feasibility of the linear matrix inequality described by (24), and it can be solved by the LMI

approach. In this paper, the linear matrix inequality (24) is feasible when γ=0.7. In the next section, the proposed hierarchical switching control system of vehicle longitudinal acceleration will be validated by simulations and experiments.

4. SIMULATION AND EXPERIMENT

To illustrate the advantages of the proposed control algorithm, simulations have been done to compare the performance of the proposed controller with that of a PID controller under different conditions. The gains of the PID controller are determined under nominal conditions

Table 2. Simulation conditions.

Index	Simulation conditions				
	Slope	Vehicle mass	Wind speed	Time constant of engine	Gear
1	0	1250	0	0.35	2
2	–0.02	1000	4	0.2	1
3	0.02	1500	–4	0.4	1
4	–0.02	1000	4	0.2	4
5	–0.02	1000	4	0.4	4
6	0.02	1500	–4	0.2	4

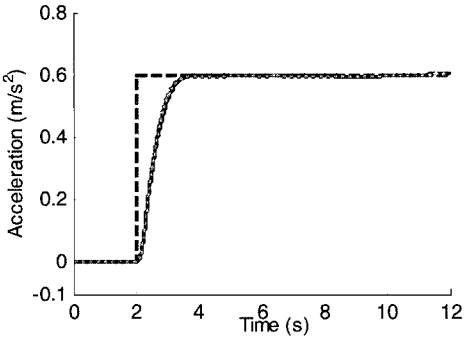

(a) Simulation results of index 1

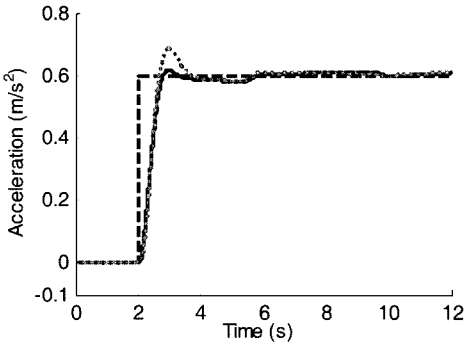

(b) Simulation results of index 2

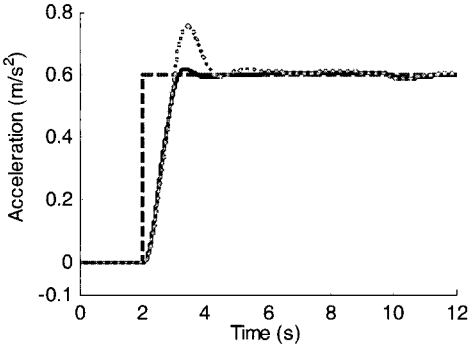

(c) Simulations results of index 3

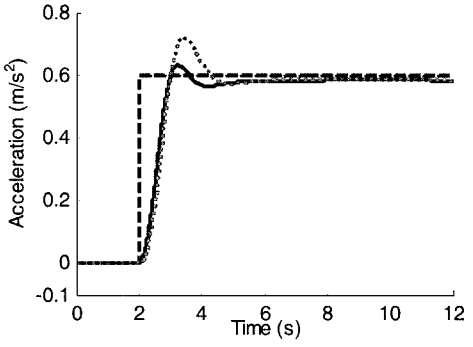

(d) Simulation results of index 4

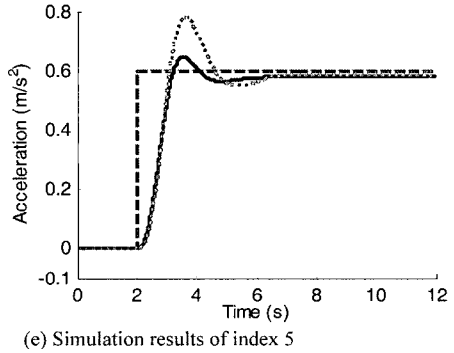

(e) Simulation results of index 5

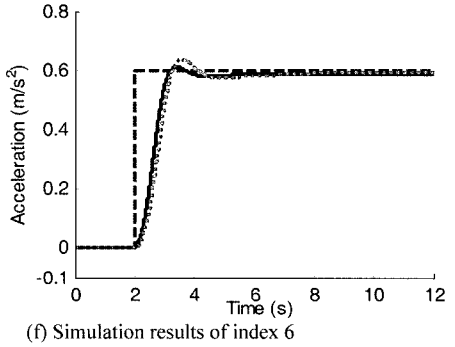

(f) Simulation results of index 6

– – Desired value, —— the proposed algorithm, ... PID controller

Figure 6. Simulation results under different conditions.

and the gains of the P, I and D terms are 1, 2 and 0.01 respectively. During the simulation, the initial speed of the vehicle is 9 m/s and the desired acceleration is a step signal of 0.6 m/s^2. Some of the results and the simulation conditions are shown in Table 2 and the results are shown in Figure 6. The values of the parameters, whose values are not given in Table 2, are set to the nominal values.

In the nominal condition, the two controllers have almost the same performance (as shown in Figure 6(a)), but when values of the vehicle and environment parameters change, the response of PID controller has a much larger overshoot than the proposed control algorithm (as shown in Figure 6(b), (c), (d), (e)). The maximum tracking error of a PID controller is up to 0.2 m/s^2 and that of the proposed algorithm is only about 0.05 m/s^2. When parameters change, the proposed algorithm adjusts the controller and the proper controller is switched into the closed loop in time. When designing the controller set in section 3.3, The robust stability and tracking ability of the closed loop system under switching are ensured. A PID controller does not have this adaptive ability. For the plant for acceleration controller design, whose dynamics chage very much under different conditions, it can hard to provide satisfactory control.

Furthermore, experiments have also been carried out to validate the performance of the control scheme. In the test, the exact values of vehicle and environment parameters are not known, but lie within the ranges shown in Table 1. Some of the results are shown in Figure 7.

The experiments include several acceleration and deceleration processes. Since braking pressure control is not considered in this study, the max deceleration only reaches about −0.4 m/s^2 and the max acceleration is about 0.6 m/s^2. A comparison between the desired acceleration a_{des} and the actual acceleration a is shown in Figure 8(a). The results show that the actual vehicle longitudinal acceleration can track the desired values rapidly and exactly. Figure 8(c) is the switching signal σ and it is shown that when the dynamics of the plant vary in the possible range, the proper controller can be selected and switched into the closed loop in time. Figure 8(d) is the response of the throttle angle, which is smooth and there are no large sudden changes when controller switchings occur. Figure 8(b) is the response of the vehicle speed.

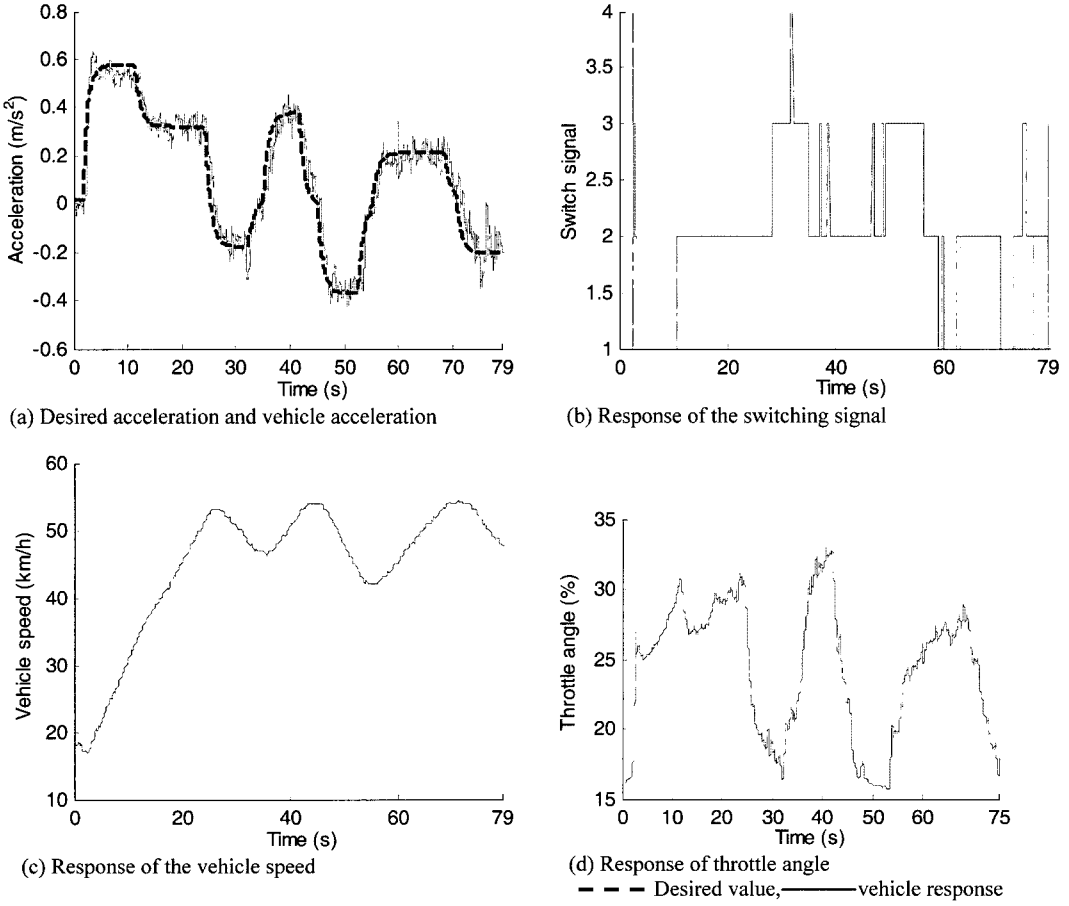

(a) Desired acceleration and vehicle acceleration

(b) Response of the switching signal

(c) Response of the vehicle speed

(d) Response of throttle angle

– – – Desired value, ——— vehicle response

Figure 7. Experiment results of the proposed acceleration tracking control algorithm.

5. CONCLUSIONS

To deal with the tracking control problem of vehicle longitudinal acceleration in the presence of large uncertainties, a hierarchical switching control system based on robust control theory is designed based on the analysis of the vehicle longitudinal dynamics. By simulation and experimental validation, it can be concluded that:

(1) The vehicle longitudinal dynamics chage very much under different conditions and a fixed-parameter controller can hard control in a satisfactory way.

(2) By the switching algorithm based on the estimation of the $L_{2\delta}$ gain of the uncertainty between the plant and the nominal models, the proper controller can be selected to control vehicle longitudinal acceleration when vehicle longitudinal dynamics change.

(3) The proposed algorithm can control vehicle acceleration well in the presence of large uncertainties. The response time is smaller than 1.5s and the maximum tracking error is only 0.05 m/s^2 with the step input.

(4) By considering the robust performance of the closed system under switching and the adaptive ability of the proposed control system, this controller demonstrates better performance than a PID controller, whose maximum tracking error is up to 0.2 m/s^2.

In this study, the state feedback approach is used to control the acceleration, which may result in jerks when switchings occur. In the next step, the output feedback approach will be considered and the sudden changes will be eliminated by some proper format of the controller set.

REFERENCES

Datta, A. (1998). *Adaptive Internal Model Control.* Springer. London. 25–26.

Hedrick, J. K. (1998). Nonlinear controller design for automated vehicle applications. *UKACC Int. Conf. Control*, 23–32.

Hespanha, J., Liberzon, D. and Morse, A. S. (2003). Hysteresis-based switching algorithms for supervisory control of uncertain systems. *Automatica*, **39**, 263–272.

Hou, D., Gao, F. and Li, K. (2003). A study on lower layer control of vehicle collision avoidance system with MMC method. *Automotive Engineering* **25**, **4**, 399–342.

Ippoliti, G. and Longhi, S. (2004). Multiple models for adaptive control to improve the performance of minimum variance regulators. *IEE Proc. Control Theory & Application* **151**, **2**, 210–217.

Kumpai, S. N. and Jeyendran, B. (1997). Adaptive control using multiple models. *IEEE Trans. Automatic Control* **42**, **2**, 171–187.

Lee, G. D. and Kim, S. W. (2002). A longitudinal control system for a platoon of vehicles using a fuzzy sliding model algorithm. *Mechatronics*, **12**, 97–118.

Li, Y. (2002). *Robust Control-LMI Approach.* Tsinghua Press. Beijing. 8.

Lu, X.-Y. and Hedrick, J. K. (2003). Longitudinal control design and experiment for heavy duty trucks. *Proc. American Control Conf.*, 36–41.

McMahon, D. H. and Hedrick, J. K. (1989). *Longitudinal Model Development for Automated Roadway Vehicles.* UCB-ITS-PRR-89-5. University of California. Berkeley.

Morse, A. S. (1996). Supervisory control of families of linear set point controllers part 1: exact matching. *IEEE Trans. Automatic Control* **41**, **10**, 1413–1431.

Rajamani, R. and Shladover, S. E. (2001). An experimental comparative study of autonomous and cooperative vehicle following control systems. *Transportation Research Part C*, **9**, 15–31.

Rong, X. Zhao, Z. and Li, X. (2005). General model set design methods for multiple model approach. *IEEE Trans. Automatic Control* **50**, **9**, 1260–1276.

St. Germann and Isermann, R. (1995). Nonlinear distance and cruise control for passenger cars. *Proc. American Control Conf.*, 3081–3085.

Yi, K. and Kwon, Y. D. (2001). Vehicle to vehicle distance and speed control using an electronic vacuum booster. *JSAE Review*, **22**, 403–412.

Yi, K. and Moon, I.-K. (2004). A driver adaptive stop and go cruise control strategy. *Proc. 2004 IEEE Int. Conf. Networking, Sensing & Control*, 601–606.